Journal of Applied Statistics

ISSN: 0266-4763 (Print) 1360-0532 (Online) Journal homepage: www.tandfonline.com/journals/cjas20

Estimation of torsion

K. V. Mardia

Journal of Applied Statistics, Vol. 26, No. 3, 1999, 373–381

Estimation of torsion

K. V. MARDIA[1], **R. J. MORRIS**[1], **A. N. WALDER**[1] **&**
J. J. KOENDERINK[2], [1]*University of Leeds, UK and* [2]*Utrecht University, The Netherlands*

ABSTRACT *Spinal deformity is a more common problem in children than is usually realized, and early diagnosis is highly desirable. One current measure of detection is quite crude, with an angle being taken by hand from X-rays. In this paper, we present some thoughts and exploratory results for assisting orthopaedic surgeons, by estimating torsion.*

1 Introduction

The torsion of a curve at a point is a number which characterizes the deviation of the curve, in a small neighbourhood that contains the point, from its osculating plane. Our work was motivated by our interest in spinal profiles. Assume that, for a set of vertebrae, we are able to calculate their centroids, so have a collection of points in three dimensions. For healthy patients, the spine line that joins these centroids should lie in a two dimensional plane (see Mardia *et al.*, 1996a). We wish to know whether or not this is the case, and will do this by estimating the torsion at these central locations. If the value is non-zero, then we have evidence of the spine line not lying in the plane and, hence, evidence of a spinal problem.

2 Estimating torsion

Let $\gamma(t)$ be a unit speed curve with tangent $\vec{\mathbf{T}} = \gamma'$ where throughout primes denote derivatives with respect to the arc length. The acceleration of the curve can be written as $\vec{\mathbf{T}}' = \kappa \vec{\mathbf{N}}$, where $\vec{\mathbf{N}}$ is a unit length vector called the 'normal' and κ is the curvature, which describes how sharply the curve bends. Because we have a unit speed curve, the normal is orthogonal to the tangent. The plane spanned by $\vec{\mathbf{T}}$ and $\vec{\mathbf{N}}$ is called the 'osculating plane'. The binormal is $\vec{\mathbf{B}} = \vec{\mathbf{T}} \wedge \vec{\mathbf{N}}$, and the torsion is

Correspondence: K. V. Mardia, Department of Statistics, School of Mathematics, University of Leeds, Leeds LS2 9JT.

0266-4763/99/030373-09 $7.00

$\tau = \vec{\mathbf{N}}' \cdot \vec{\mathbf{B}}$. We can only define the normal and binormal when $\vec{\mathbf{T}}'$ is non-zero, i.e. when the curvature is non-zero. We have

$$\begin{aligned} \vec{\mathbf{T}}' &= \kappa \vec{\mathbf{N}}, \\ \vec{\mathbf{N}}' &= \tau \vec{\mathbf{B}} - \kappa \vec{\mathbf{T}}, \\ \vec{\mathbf{B}}' &= -\tau \vec{\mathbf{N}}, \end{aligned}$$

the Serret–Frenet equations (see Koenderink, 1990, Section 5.2). These definitions are for a continuous curve; we now move on to consider approximations to them in the discrete case.

2.1 *Method 1*

Assume that we have a set of n points in three dimensions, $\mathbf{X}_i = (x_i, y_i, z_i)$, where z_i has special importance—in this case, height. We difference consecutive points, and normalize by their change in height:

$$\mathbf{Y}_i = \left(\frac{x_{i+1} - x_i}{z_{i+1} - z_i}, \frac{y_{i+1} - y_i}{z_{i+1} - z_i} \right), \qquad i = 1, \ldots, n-1.$$

A plot of the $\mathbf{Y}_i$ terms is a plot of the tangent space of the spherical image in the positive z-direction. At every point, the unit tangent to the line is a point of the surface of a sphere (the 'spherical image'). The arc length of the spherical image is related to the original line's curvature, and the curvature of the spherical image is related to the torsion (sometimes called the 'second curvature') of the line. From it, we can estimate its curvature K, by taking sets of five points, translating the middle point to the origin, and fitting the quadratic $ax^2 + bx$. Using the curvature formula

$$\frac{\mathrm{d}^2 y/\mathrm{d}x^2}{[(\mathrm{d}y/\mathrm{d}x)^2 + 1]^{3/2}}$$

the curvature K of the spherical image is given by

$$K = \frac{2a}{[(2ax + b)^2 + 1]^{3/2}}$$

calculated at $x = 0$. Further, if we let $\mathrm{d}s_i = \|\mathbf{X}_i - \mathbf{X}_{i-1}\|$ and $\mathrm{d}\theta_i = \|\mathbf{Y}_i - \mathbf{Y}_{i-1}\|$, then the curvature κ of the space curve is given by

$$\kappa = \frac{\mathrm{d}\theta}{\mathrm{d}s}$$

and the torsion τ is given by

$$\tau = \kappa K.$$

For a discussion of these geometric concepts, see, for example, Koenderink (1990, pp. 179–183).

2.2 *Method 2*

As will be seen from the example on the helix in Section 4, the preceding method of estimating torsion seems to overestimate somewhat. Instead of projecting on to a plane normal to the z-axis, we now project on to a plane normal to the tangent direction. Let

$$\vec{\mathbf{T}}_i = c_i(x_{i+1} - x_i, y_{i+1} - y_i, z_{i+1} - z_i), \qquad i = 1, \ldots, n-1$$

be the normalized tangent directions, with c_i such that $|\vec{\mathbf{T}}_i| = 1$. At a specific point k, we have its tangent direction $\vec{\mathbf{T}}_k$, and can calculate a unit vector $\vec{\mathbf{N}}_k$ normal to it and the x-axis, and another unit vector $\vec{\mathbf{B}}_k$ normal to both $\vec{\mathbf{T}}_k$ and $\vec{\mathbf{N}}_k$. The unit distance tangents around point k can be written as

$$\frac{1}{\vec{\mathbf{T}}_i \cdot \vec{\mathbf{T}}_k}\vec{\mathbf{T}}_i = \vec{\mathbf{T}}_k + \frac{\vec{\mathbf{T}}_i \cdot \vec{\mathbf{N}}_k}{\vec{\mathbf{T}}_i \cdot \vec{\mathbf{T}}_k}\vec{\mathbf{N}}_k + \frac{\vec{\mathbf{T}}_i \cdot \vec{\mathbf{B}}_k}{\vec{\mathbf{T}}_i \cdot \vec{\mathbf{T}}_k}\vec{\mathbf{B}}_k,$$

$$i = k-2, \ldots, k+2$$

Hence, we can consider the plane curve

$$\left(\frac{\vec{\mathbf{T}}_i \cdot \vec{\mathbf{N}}_k}{\vec{\mathbf{T}}_i \cdot \vec{\mathbf{T}}_k}, \frac{\vec{\mathbf{T}}_i \cdot \vec{\mathbf{B}}_k}{\vec{\mathbf{T}}_i \cdot \vec{\mathbf{T}}_k}\right)$$

to give local pictures of the spherical image. From these local pictures, calculate K and then treat their midpoints ($i = k$) as $\mathbf{Y}_i$ terms to obtain κ, and then τ.

3 Computation

A little care is needed in practice, because each of the computed variables has a different number of values, and how they are actually paired up and calculated is important. For n points, originally there will be n $\mathbf{X}_i$, $(n-1)\mathbf{Y}_i$ or $\vec{\mathbf{T}}_i$, $(n-5)K$, $(n-1)\mathrm{d}s_i$, and $(n-2)\mathrm{d}\theta_i$. Interpolating $n-3$ intermediate values of the $\mathrm{d}\theta_i$ terms gives a possible way of pairing things up, using all values of K, and the central $n-5$ values of $\mathrm{d}s$ and the (interpolated) $\mathrm{d}\theta$.

4 Examples

4.1. Helix

We first tried estimating the torsion for a helix $(x, y, z) = (a \cos t, a \sin t, t)$. This is almost the simplest parameterized version of the helix. It lies in three dimensions on the surface of the cylinder $x^2 + y^2 = a^2$, and winds around it in such a way that, when t increases by 2π, both x and y return to their original values, while z increases by 2π, i.e. the pitch of the helix. This has both constant curvature $a/(a^2+1)$ and constant torsion $1/(a^2+1)$. For t in the range $[0, 2\pi]$, $n = 21$ equispaced points lying on the helix were first used to calculate the torsion (as given in Table 1) and also the curvature (as given in Table 2).

TABLE 1. True and estimated values of torsion for the two approaches

		Estimated value	
a	True	Method 1	Method 2
0.1	0.99	1.09	1.08
0.5	0.8	0.98	0.85
1	0.5	0.78	0.50
2	0.2	0.49	0.19
5	0.04	0.22	0.04

TABLE 2. True and estimated values of curvature for the two approaches

a	True	Estimated value Method 1	Estimated value Method 2
0.1	0.099	0.098	0.098
0.5	0.400	0.444	0.397
1	0.500	0.703	0.498
2	0.400	0.890	0.399
5	0.192	0.976	0.192

We observe from both these tables that Method 2 performs much better than does Method 1.

Increasing the number of points for Method 1 brings the estimated torsion closer to the true value. The computation here is not a problem because K, $d\theta$ and ds are all constant, so just one value for torsion is given for each helix.

4.2 *Spines*

From two orthogonal X-rays, we were able to locate approximate three-dimensional vertebrae centres, and were looking for ways to classify spinal shape (see Walder *et al.*, 1998). Typically, this would give us 12 points in three dimensions, from the fifth thoracic vertebra to the fourth lumbar. Here, x was front–back, y left–right and z height.

In Fig. 1, we show the lateral and frontal views of the approximate locations of the vertebrae centres of a healthy spine, as obtained from X-rays. In Fig. 1(c), we have its spherical image calculated via Method 1: the fact that, in Fig. 1(c), the plot is nearly horizontal indicates that we have a straight spine, with approximately zero torsion. (A straight line means that all the curvature lies in a vertical plane; the line being horizontal means that the plane is $y=$ constant.) For 12 points on

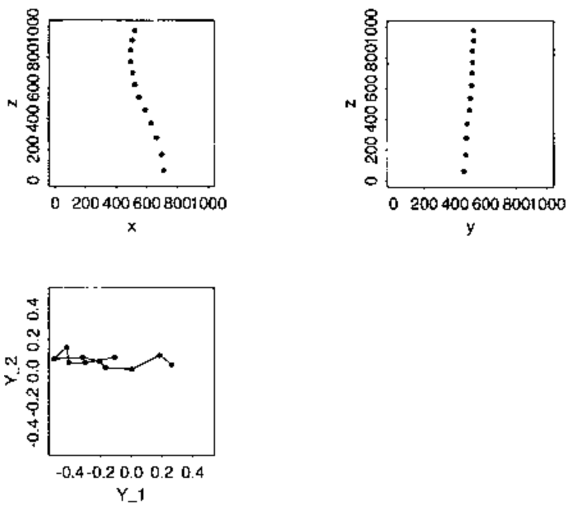

FIG. 1. (a) Lateral spine profile, (b) frontal profile and (c) spherical image (Method 1).

TABLE 3. Values of torsion estimated by the two methods for a healthy spine

	Torsion ($\times 10^{-3}$)						
Method 1	2.112	3.633	0.510	6.752	3.114	6.369	0.850
Method 2	2.090	3.547	0.465	6.503	2.912	7.122	0.962

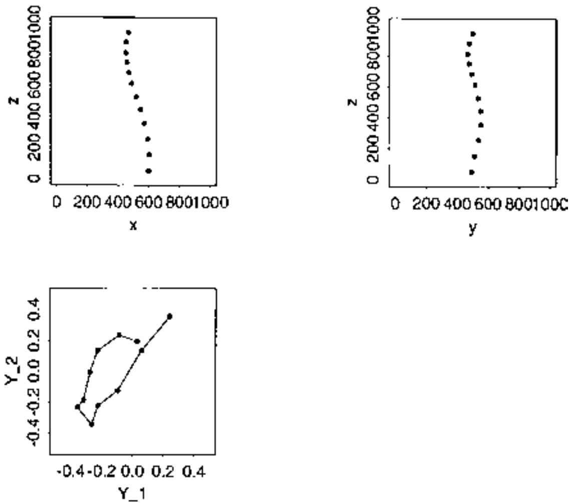

FIG. 2. (a) Lateral spine profile, (b) frontal profile and (c) spherical image (Method 2).

TABLE 4. Values of torsion estimated by the two methods for a scoliotic spine

	Torsion ($\times 10^{-3}$)						
Method 1	0.896	10.867	19.916	2.810	79.908	1.124	1.574
Method 2	0.967	10.324	20.959	2.036	12.142	1.016	1.682

the spine, we have seven estimated torsion values; the results are similar for both methods. They are probably not significantly different from zero, as required (see Table 3).

In contrast, Fig. 2 is of a scoliotic spine (note the non-straight frontal profile). Its spherical image is clearly not straight, and we would expect non-zero torsion. Table 4 has similar values for both methods, but this time note that some of the values are much larger than those we obtained in Table 3. These values are probably significantly different from zero.

Note that it is possible for a severely deformed spine to have most of its spine line points lying in a (vertical) plane. However, when viewed from the front, the spinal profile is not straight, as in this case, and the vertical plane is not of the form $y =$ constant. This is a clear indication of a spinal problem, and would be picked up by non-zero torsion values in our calculations.

Also note that the curve appears to consist of two planar arcs with distinct osculating planes (probably joined at the curvature zero). For an alternative way of analyzing spinal shape, see Mardia *et al.* (1996b) and Mardia *et al.* (1999).

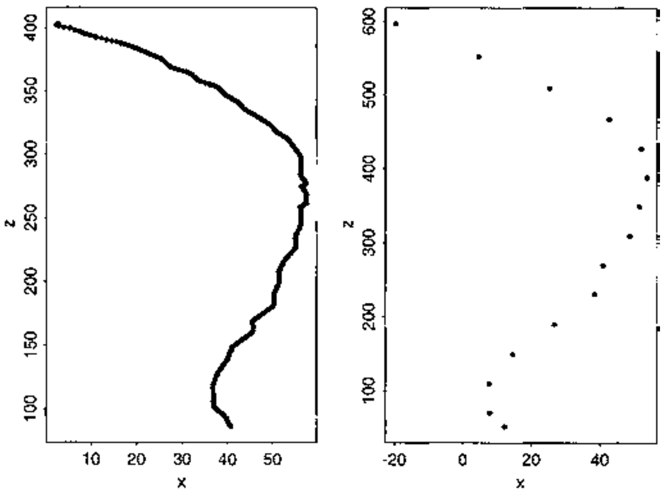

FIG. 3. Lateral spine profile for (a) original data and (b) reduced data.

5 Quantec data

We also have Quantec data available: a white-light scanning system which can give in the region of 400 points that correspond to the exterior spinal profile. There are far too many points with which to work but, using a subset of these data, we could calculate torsion as described already and again classify spinal shape as follows.

(1) Kent *et al.* (1983) provide an approach and an algorithm for taking a set of (ordered) three-dimensional points and finding the (unknown number of) linear segments which best fit the points. (See also, Kanatani, 1993, pp. 351–3.)
(2) The first eigenvector could be obtained via principal component analysis (PCA) for each segment. Adding the eigenvectors together (after multiplying each by their corresponding eigenvalue) would given an approximate representation of the spine.
(3) Cumulative sums of the eigenvectors, could then give a much reduced set of points to analyze.

In Figs 3 and 4, we simplify step (1) as just described, and simply divide the Quantec data into (say) 15 sets, each containing approximately the same number of points. PCA is performed on each subset, and the first eigenvectors (scaled by their corresponding eigenvalues) have been summed together. In Fig. 3, we have the lateral profiles, with Fig. 3(a) showing the original data and Fig. 3(b) showing the reduced data from the scaled, summed eigenvectors. Similarly, in Fig. 4, the data are shown for the frontal profiles. (The data do not lie in one straight line, because of a problem with the data capture. However, note that the very different scales on the axes accentuate what is only a small problem.) The points in Figs 3(b) and 4(b) provide a good summary of the original data, and can now be used in the previous torsion calculations.

When we applied the methods just described to two sets of Quantec data, our earlier results were confirmed. For a straight spine consisting of 354 points, the two methods estimated the maximum torsion values to be 0.0020 and 0.0021

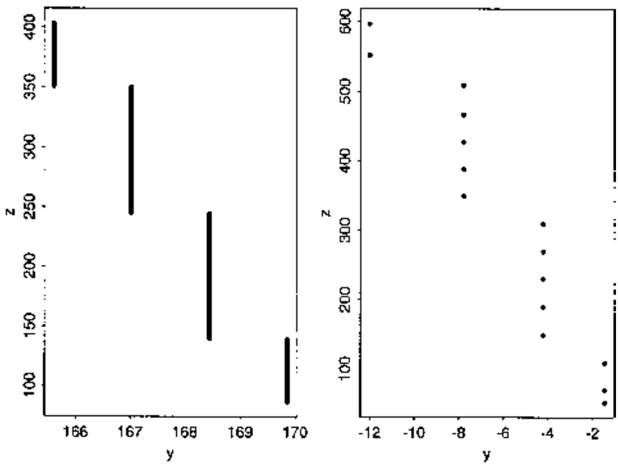

FIG. 4. Frontal spine profile for (a) original data and (b) reduced data.

respectively. For a scoliotic spine consisting of 245 points, the methods estimated the maximum values of torsion to be 0.0572 and 0.0430. Again, we see that the second two values are larger; taking logarithms of the torsion would highlight this difference better. (Although we are not told the units of measurements, torsion has the physical dimension of reciprocal length.)

6 An alternative torsion measure

If we have a curve $\gamma(t)$ lying on a surface with unit normals $\vec{\mathbf{S}}$, then we can consider an alternative torsion measure (see, for example, Koenderink, 1990, Section 6.1). As before, let $\vec{\mathbf{T}}$ be the unit length tangent to the curve. Let $\vec{\mathbf{V}} = \vec{\mathbf{S}} \wedge \vec{\mathbf{T}}$. This lies in the tangent plane to the surface and is called the 'hinge direction'. The derivatives of $\vec{\mathbf{T}}$, $\vec{\mathbf{V}}$ and $\vec{\mathbf{S}}$ are related by

$$
\begin{aligned}
\vec{\mathbf{T}}' &= \kappa_g \vec{\mathbf{V}} + \kappa_n \vec{\mathbf{S}}, \\
\vec{\mathbf{V}}' &= \tau_g \vec{\mathbf{S}} - \kappa_g \vec{\mathbf{T}}, \\
\vec{\mathbf{S}}' &= -\kappa_n \vec{\mathbf{T}} - \tau_g \vec{\mathbf{V}},
\end{aligned}
$$

where κ_n is the normal curvature, κ_g is the geodesic curvature and τ_g is the geodesic torsion. If ϕ is the angle between the binormal $\vec{\mathbf{B}}$ and the surface normal $\vec{\mathbf{S}}$, then $\kappa_g = \kappa\cos(\phi)$, $\kappa_n = \kappa\sin(\phi)$ and $\tau_g = \tau - \phi'$ (Fig. 5). In other words, κ_n describes

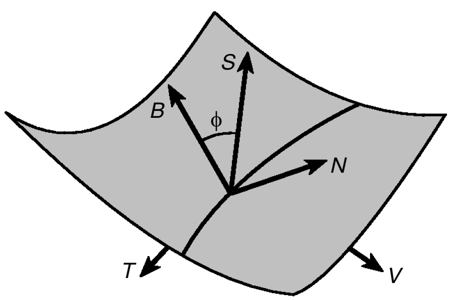

FIG. 5. Relationship between the $\vec{\mathbf{T}}\vec{\mathbf{N}}\vec{\mathbf{B}}$ and $\vec{\mathbf{T}}\vec{\mathbf{V}}\vec{\mathbf{S}}$ frames.

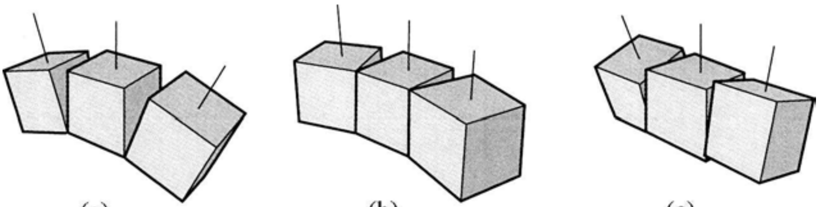

FIG. 6. The three types of variation: (a) $\kappa_n \neq 0$, $\kappa_g = 0$, $\tau_g = 0$; (b) $\kappa_n = 0$, $\kappa_g \neq 0$, $\tau_g = 0$; (c) $\kappa_n = 0$, $\kappa_g = 0$, $\tau_g \neq 0$.

the amount of curvature in the surface normal direction, κ_g describes the amount of curvature within the surface tangent plane and τ_g describes how the surface twists. This is related to the curve torsion and the rate of change of the angle between $\vec{\mathbf{S}}$ and $\vec{\mathbf{N}}$.

For curves that lie on a surface, as in the case of spines, these are possibly more natural measures. Figure 6 depicts three situations for spines, where just one of these numbers is non-zero. The blocks represent individual vertebrae with the normals to the backs indicated by an arrow.

If we have the data for the points on a spine, which include data for the unit normals, then we can use techniques similar to those in the previous sections to provide estimates for κ_n, κ_g and τ_g. Both κ_g and τ_g may prove useful for distinguishing scoliotic spines. Such data will arise when the Quantec data are not preprocessed, and when two orthogonal X-ray views are available for the spine. However, this approach will require appropriate discretization, as in the previous cases. For example, to find a normal to a point on a curve in three dimensions, find the principal components of a collection of points nearby, and the direction of the maximum variation will be the required normal.

7 Discussion

At this point, we have a method of estimating torsion as given in Section 2.2 (Method 2), which performs well on various helices, and would appear to be able to differentiate between straight and scoliotic spines—although more rigorous testing of this is obviously required. Some other ways in which we could proceed are given in Ramsay & Silverman (1997). For example, we could use spline estimates of derivatives (p. 60), or kernel estimates (p. 53).

Acknowledgements

We are grateful to the EPSRC for a visiting fellowship provided to Professor Koenderink.

REFERENCES

KANATANI, K. (1993) *Geometric Computation for Machine Vision* (Oxford, Clarendon Press).

KENT, J. T., BRIDEN, J. C. & MARDIA, K. V. (1983) Linear and planar structure in ordered multivariate data as applied to progressive demagnetization of paleomagnetic remanence, *Geophysical Journal of the Royal Astronomical Society*, 75, pp. 593–621.

KOENDERINK, J. J. (1990) *Solid Shape* (Cambridge, MA, MIT Press).

MARDIA, K. V., BACZKOWSKI, A. J., FENG, X. & MILLNER, P. A. (1996a) A study of three-dimensional curves, *Journal of Applied Statistics*, 23, pp. 139–148.

MARDIA, K. V., WALDER, A. N., MILLNER, P. A., BERRY, E. & DICKSON, R. A. (1996b) Analysis of 3D spinal shape from two x-ray views, *Proceedings of Image Fusion and Shape Variability Techniques*, pp. 123–128 (Leeds University Press).

MARDIA, K. V., WALDER, A. N., BERRY, E., DICKSON, R. A., MILLNER, P. A. & SHARPLES, D. (1999) Assessing spinal shape, *Journal of Applied Statistics*, 26(7), forthcoming.

RAMSAY, J. O. & SILVERMAN, B. W. (1997) *Functional Data Analysis* (New York, Springer).